Magnetically Targeted Endothelial Cells for Prevention of Vascular Restenosis

Boris Polyak[*✉], Mikhail Medved[*], Nina Lazareva[*], Lindsay Steele[*], Tirth Patel[*], Ahmad Rai[*], Menahem Y. Rotenberg[**], Kimberly Wasko[*], Andrew R. Kohut[*], Richard Sensenig[***], Gennady Friedman[*]

*Drexel University, Philadelphia, PA 19102, USA; ✉bpolyak@drexelmed.edu
[**]Ben-Gurion University of the Negev, Beer-Sheva, 84105, Israel
[***]University of Pennsylvania, Philadelphia, PA 19104, USA

ABSTRACT

The present study assessed the potential of magnetically mediated delivery of endothelial cells (ECs) to inhibit in-stent stenosis induced by mechanical injury in a rat carotid artery stent angioplasty model. Syngeneic ECs loaded with polymeric magnetic nanoparticles (MNPs) were administered at the distal end of the stented artery using a brief exposure (12 min) to a uniform magnetic field (1.4-kOe). After two months, magnetic localization of ECs demonstrated significant protection from stenosis at the distal part of the stent in the cell therapy group compared to both the proximal part of stent in the cell therapy group and the control (stented, nontreated) group: 1.7-fold ($p < 0.001$) less reduction in lumen diameter as measured by B-mode and color Doppler ultrasound, 2.3-fold ($p < 0.001$) less reduction in the ratios of peak systolic velocities as measured by pulsed wave Doppler ultrasound, and 2.1-fold ($p < 0.001$) attenuation of stenosis as determined through end point morphometric analysis.

Keywords: in-stent restenosis, endothelium, cell therapy, magnetic targeting, vascular healing.

1 INTRODUCTION

Over the past decade, the advent of percutaneous transluminal angioplasty with stent implantation and the even more recent use of drug-eluting stents have resulted in a paradigm shift in the care of obstructive vascular disease[1]. However, deleterious sequelae of endovascular interventions are the result of unavoidable mechanical damage to the vessel wall. Disruption of the endothelial monolayer exposes the underlying media and induces a cascade of cellular and biological events, resulting in abnormal vascular wall function[2].

Current standards of clinical care focus on inhibition of smooth muscle cells using drug-eluting stents that release nonselective antiproliferative drugs, which also affect ECs, the important modulators of vascular hemostasis, fibrinolysis, and proliferative state of the smooth muscle cells. Alternatively, the promotion of healing in the vascular endothelium may be a more natural and consequently safer approach in the prevention of vascular restenosis and thrombosis. Therefore, strategies that promote recovery of ECs in the vessel wall following injury may limit complications such as thrombosis, vasospasm, and neointimal formation, through the reconstitution of a luminal barrier and cellular secretion of paracrine factors[3].

Magnetic targeting of ECs to the vessel wall is a promising technique that has been applied to address the reendothelialization and subsequent healing of the injured blood vessels. The feasibility of magnetic localization of ECs to stented blood vessels has been demonstrated using transiently[4] and permanently[5] magnetized vascular stents. Recently, magnetic delivery of ECs to transiently magnetized stents in a rat carotid stenting artery model have shown to result in enhanced capture, retention, and proliferation of ECs at the site of stent implantation[6]. Circumferential magnetic delivery of ECs overexpressing endothelial nitric oxide synthase (eNOS) in the non-stented vessel has shown to improve vascular function after mechanical injury in a mouse carotid artery injury model[7]. A circular Halbach array, which augments the magnetic field at its center, was used to demonstrate an increase in cell retention in non-stented vessels leading to a non-significant reduction of restenosis three weeks after cell delivery in a rabbit model[8]. These studies provide encouraging indications that magnetic targeting of ECs can offer an effective way to accelerated recovery of denuded endothelium in blood vessels and potentially mitigate pathological side-effects associated with a mechanical injury after implantation of endovascular stents.

In the present study, we assessed the potential of magnetically guided delivery of syngeneic ECs to inhibit experimental in-stent stenosis induced by mechanical injury in a rat carotid artery stent angioplasty model.

2 MATERIALS AND METHODS

2.1 Nanoparticles and cell preparation

Polylactide-based magnetic nanoparticles were formulated with the inclusion of nanocrystalline magnetite by a modified emulsification-solvent evaporation method as described elsewhere[9]. The particles contained 48.2±1.32% (w/w) magnetite and had a mean hydrodynamic diameter of 278±1.62nm and ζ-potential of -14.4±0.34mV. The magnetization of the MNPs measured at 0.5T was 24.6±1.22emu/g of the composite. Full physicochemical characterization of MNPs can be found in[9].

Rat aortic endothelial cells (RAEC) were isolated and characterized according to previously published protocol[10]. For cell loading, 300,000-350,000 RAECs were seeded on clear bottom 12-well plates using MCDB 131 medium supplemented with 5% Fetal Bovine Serum (FBS), Epidermal Growth Factor (EGF) (10ng/ml), Hydrocortisone (1µg/ml) and L-Glutamine (10mM) and incubated with MNP suspension at a dose of ~100pg magnetite/cell at 37^{o}C overnight on a 96-well magnetic separator with surface force density of 66T^{2}/m (LifeSep 96F, Dexter Magnetic Technologies, USA). The magnetite content within RAECs was estimated to be 25.3±0.75pg magnetite/cell as quantified by the method described elsewhere.[11]

2.2 Stent angioplasty and *in vivo* cell delivery

A complete description of the surgical procedure and cell delivery methodology can be found in the literature[12]. Briefly, under general anesthesia left common carotid arteries along with external and internal carotids were isolated with blunt dissection. The external carotid was permanently ligated as distal as possible. The proximal part of the common carotid and internal carotid were temporarily occluded with vascular clip and temporary ligature respectively. Injury of common carotids was induced with four passages of 2F Fogarty embolectomy catheter (Edwards Lifesciences, Irvine, CA, USA). A 304-grade stainless steel stent (Laserage Technology Corp. Waukegan, IL, USA) was introduced into common carotid through the conductor tube inserted in external carotid and deployed at the injured artery segment with angioplasty balloon catheter (NuMED Inc., Hopkinton, NY, USA). In control animals (n=13), the procedure was completed with permanent ligation of the external carotid distal to the common carotid bifurcation, blood flow restored and wound closed. In cell delivery animals (n=13), a 100µL of 3×10^{3} cells/ µL were injected at a rate 50µL/min exposing the animal to a uniform magnetic field of 0.14T generated across the neck area by two symmetrical electromagnets for 12min.

2.3 Imaging and morphometric analysis

The therapeutic effect of magnetically targeted cell therapy was assessed by ultrasonic brightness (B-mode), color Doppler and spectral (pulsed wave) Doppler imaging measuring morphological (lumen diameter) and hemodynamic (peak systolic velocity) changes in the targeted and non-targeted (control) animals using Vevo®2100 Imaging System (VisualSonics Toronto, ON, Canada)[12].

During the necropsies (64±1day post cell delivery) the stented arteries were fixed *in situ* by perfusion with 10% neutral buffered formalin and glycol methacrylate embedded (JB-4, Electron Microscopy Sciences, PA, USA). Serial 5-µm cross sections were stained with Verhoeff-van Gieson elastin stain or Prussian blue staining with nuclear fast red as a counterstain. The morphometric analysis was performed using Image J software (version 1.43, NIH) by an observer blinded to the study groups as described elswhere[12].

3 RESULTS AND DISCUSSION

The progression of treatment of injured arteries with magnetically delivered ECs was monitored by high frequency ultrasound imaging measuring morphological (lumen diameter of the vessel with blood flow confirmed using B-mode and color Doppler flow imaging) and hemodynamic changes (peak systolic velocity (PSV), measured by quantitative pulsed wave Doppler mode) at the proximal and distal part of the stent. Animals with stented, mechanically injured arteries without cell delivery were used as a control. Before the injury, the normal diameters of the right carotid artery (used as internal control) and left carotid artery (implanted with a stent) were 1.09±0.05 and 1.08±0.04 mm, respectively (n=26). Immediately after injury, the right carotid artery showed a transient drop in diameter, recovering to its nearly normal value with a non-significant 3% increase (P>0.05) corresponding to 1.12±0.04 mm two months later (Figure 1A). The transient drop in diameter could be a result of posttraumatic injury and effect of inflammation mediators (thromboxanes), while the subsequent increase seems to be a compensatory response due to decreased blood flow through the left common and external (permanently ligated) carotid artery. At the distal part of the stent, the control group showed marked ~22% reduction of luminal diameter, narrowing artery lumen to 0.85±0.05 mm, while the diameter reduction in the cell therapy group was more moderate ~13%, resulting in luminal narrowing to 0.95±0.04 mm after two months (Figure 1A).

Contrastingly, quantitative analysis of the luminal diameter change at the proximal part of the stent did not show statistically significant differences in luminal narrowing between the cell therapy and control groups (P>0.05) (Figure 1B). These results show selective 1.7-fold (P<0.001) greater protection from restenosis at the distal part of the stent in the cell therapy group comparing to the proximal part of the stent.

Quantitative blood flow evaluation was based on pulsed wave Doppler measurement of peak systolic velocity (PSV), a hemodynamic parameter inversely proportional to the vessel's diameter in the power of four per corollary to the Poiseuille's law. The normal PSV in the right and left carotid arteries were 937±103 and 936±150 mm/s, respectively (n=26) (Figure 1C). In clinical practice, the absolute velocities in the internal common carotid (ICA) are usually normalized to the corresponding velocities in the ipsilateral common carotid artery (CCA) by generating ICA/CCA ratios. Such ratios are theoretically more robust measures because they may compensate for differences in clinical or physiological factors such as the presence of tandem lesions, blood pressure, contralateral high-grade stenosis, hyperdynamic cardiac state, or low cardiac output.

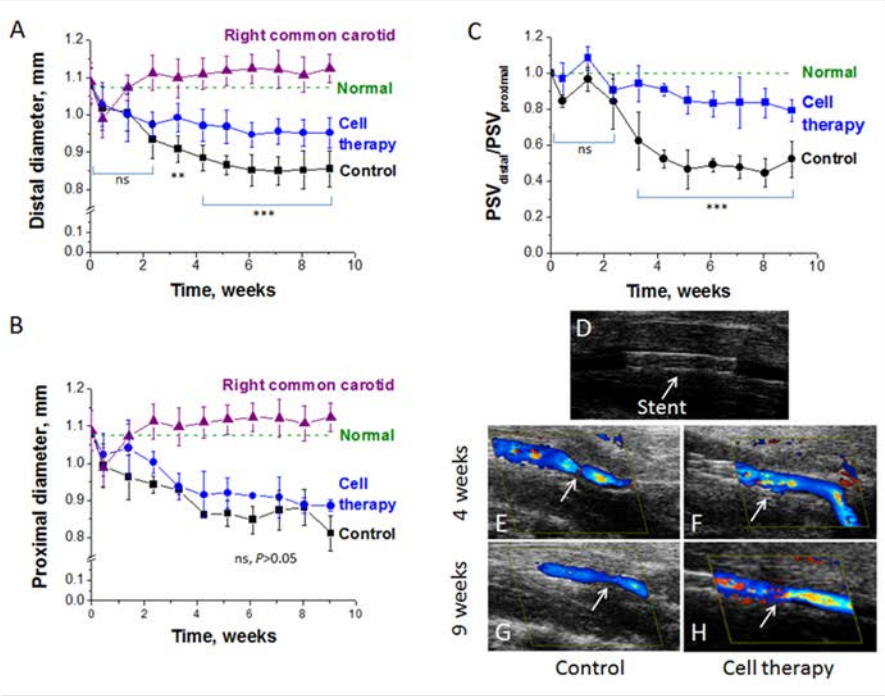

Figure 1: The protection from in-stent stenosis by the magnetically targeted EC to the stented arteries assessed by the ultrasound. (**A, B**) Changes in diameter of the stented artery at the distal and proximal end, respectively (n≥11). (**C**) Ratios of the peak systolic velocity (PSV) at the distal to proximal ends in studied animal groups (n≥11). (**D**) B-mode ultrasound image of the stented left carotid artery. (**E-H**) Representative color Doppler images of the stented arteries at different time points. Arrows indicate distal end of the stented artery segment. Data represent the means ±SD. Data comparisons were made using one-way ANOVA with Tukey's post hoc test. $^{**}P<0.01$ and $^{***}P<0.001$ *versus* untreated (control) arteries; ns, non-significant, $P>0.05$. Normal are the values measured prior to stent implantation. Reprinted with permission from Polyak, B.; Medved, M.; Lazareva, N.; Steele, L.; Patel, T.; Rai, A.; Rotenberg, M. Y.; Wasko, K.; Kohut, A. R.; Sensenig, R.; Friedman, G. Magnetic Nanoparticle-Mediated Targeting of Cell Therapy Reduces In-Stent Stenosis in Injured Arteries. *ACS Nano* 2016, 10 (10), 9559–9569. Copyright (2016) American Chemical Society.

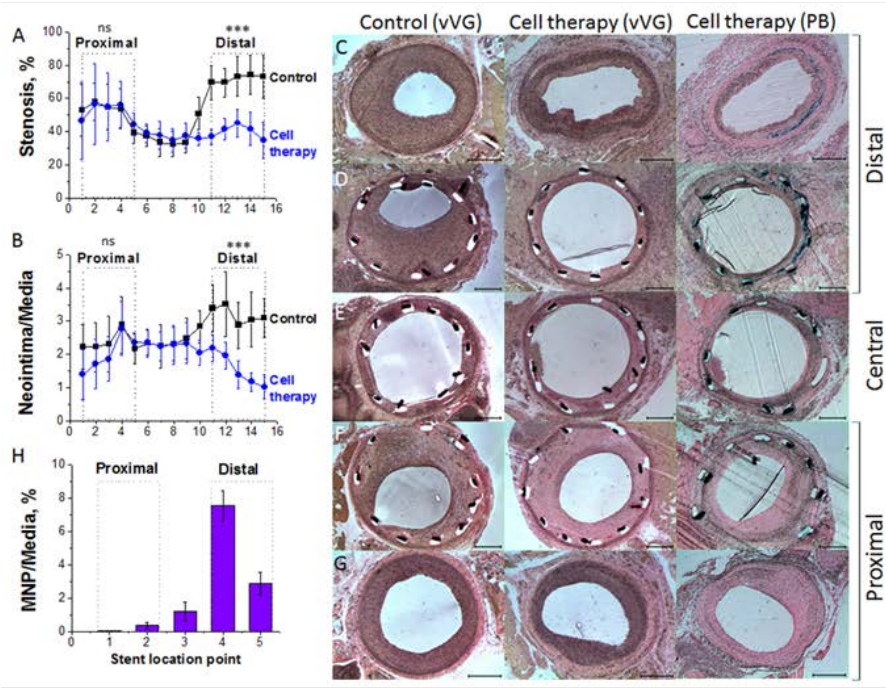

Figure 2: The protection from in-stent stenosis by the magnetically targeted EC to the stented arteries assessed by morphometric analysis. The results expressed as (**A**) percent of stent stenosis and (**B**) neointima/media ratios along the stent (n≥11). (**C-G**) Representative Verhoeff-van Gieson (vVG) and Prussian blue (PB) with nuclear fast red as counterstain sections of stented arteries in control and cell therapy group at different stent location points, respectively. Blue staining in the Prussian blue-stained histological slices indicate presence of MNPs in the vessel wall. (**H**) Distribution of the MNPs along the stented artery segment quantified from the Prussian blue-stained histological slices. The scale is 0.25mm. Data represent the means ±SD. Data comparisons were made using two-tailed unpaired Student's *t*-test. $^{***}P<0.001$ *versus* untreated (control) arteries; ns, non-significant, $P>0.05$. Reprinted with permission from Polyak, B.; Medved, M.; Lazareva, N.; Steele, L.; Patel, T.; Rai, A.; Rotenberg, M. Y.; Wasko, K.; Kohut, A. R.; Sensenig, R.; Friedman, G. Magnetic Nanoparticle-Mediated Targeting of Cell Therapy Reduces In-Stent Stenosis in Injured Arteries. *ACS Nano* 2016, 10 (10), 9559–9569. Copyright (2016) American Chemical Society.

Following this clinical standard, we compared ratios of $PSV_{distal}/PSV_{proximal}$ for each group, which represent ratios of velocities of the distal to proximal parts of the stented artery segment. The PSV ratios clearly indicate superior patency of the stented arteries in the cell therapy group, showing ~21% reduction from the normal ratio *versus* much more pronounced decrease to ~48% in PSV ratio in untreated, control group (Figure 1C). These results correlate well with the diameter changes showing 2.3-fold ($P<0.001$) greater protection from restenosis in the cell therapy group. Throughout the study, there were no episodes of stent thrombosis, and all the stented arteries remained patent to various degrees before euthanasia, as observed by the color Doppler flow imaging (Figure 1E-H).

Morphometric analysis showed that at the proximal and central part of the stented artery, the intimal area was not statistically different (P>0.05) between cell therapy and control animals as shown by percentage of stenosis (Figure 2A), neointima/media ratio (Figure 2B) and qualitative histological images (Figure 2E-G). However, at the distal part of the stented artery, cell delivery resulted in significant inhibition of in-stent stenosis with a prominent 1.8-fold (P<0.0001) reduction in the percentage of stenosis (40±1% *vs.* 72±11%) and 2.3-fold (P=0.0002) reduction in the neointima/media ratio (1.54±0.38 *vs.* 3.18±0.76) in cell therapy and control group, respectively (Figure 2A, B), which is also shown on the qualitative histological images (Figure 2C, D).

It is noteworthy that in control animals the greatest degree of stenosis was observed at the proximal and distal stent parts (edges) compared to the central part per both percentage of stenosis and neointima/media ratio. Moreover, in control animals, the trend for the significantly greater degree of stenosis was observed at the distal part of the stent comparing to the proximal part resulting in a percentage of stenosis of 72±11% and 52±12% (P=0.002) or neointima/media ratio of 3.18±0.76 and 2.36±0.16, (P=0.002) respectively. Consistently with morphometric and ultrasound data, the traces of iron oxide nanoparticles were largely found in the distal part of the stented artery per quantitative Prussian Blue (PB) staining, confirming selective localization of the delivered cells at the distal part of the stent (Figure 2C-E, cell therapy (PB) panel).

4 CONCLUSION

This work demonstrates that magnetically mediated targeting of nonmodified endothelial cells prevented the development of in-stent stenosis nearly 2-fold earlier and with a 2-fold greater magnitude at the site of successful cell delivery (distal part of the stent) in treated animals in comparison to untreated controls. In the future, addressing uniformity of cell delivery, choice of stent material, cell source and considering enhancement of EC function *via* genetic manipulation, the methodology investigated here may provide the basis for designing the next generation of cell-based therapy for vascular healing after stent angioplasty.

5 ACKNOWLEDGMENTS

This work was supported by the National Heart, Lung, and Blood Institute Award R01HL107771, W.W. Smith Charitable Trust Award H1504, Drexel University College of Medicine Clinical & Translational Research Institute (CTRI), and 2016-2017 Commonwealth of Pennsylvania Universal Research Enhancement (CURE) grant to B. Polyak.

REFERENCES

[1]. Stefanini, G. G.; Holmes, D. R., Jr. Drug-eluting coronary-artery stents. *The New England journal of medicine* 2013, 368, 254-65.

[2]. Chaabane, C.; Otsuka, F.; Virmani, R.; Bochaton-Piallat, M. L. Biological responses in stented arteries. *Cardiovascular research* 2013, 99, 353-63.

[3]. Kipshidze, N.; Dangas, G.; Tsapenko, M.; Moses, J.; Leon, M. B.; Kutryk, M.; Serruys, P. Role of the endothelium in modulating neointimal formation: vasculoprotective approaches to attenuate restenosis after percutaneous coronary interventions. *J Am Coll Cardiol* 2004, 44, 733-9.

[4]. Polyak, B.; Fishbein, I.; Chorny, M.; Alferiev, I.; Williams, D.; Yellen, B.; Friedman, G.; Levy, R. J. High field gradient targeting of magnetic nanoparticle-loaded endothelial cells to the surfaces of steel stents. *Proc Natl Acad Sci U S A* 2008, 105, 698-703.

[5]. Pislaru, S. V.; Harbuzariu, A.; Gulati, R.; Witt, T.; Sandhu, N. P.; Simari, R. D.; Sandhu, G. S. Magnetically targeted endothelial cell localization in stented vessels. *J Am Coll Cardiol* 2006, 48, 1839-45.

[6]. Adamo, R. F.; Fishbein, I.; Zhang, K.; Wen, J.; Levy, R. J.; Alferiev, I. S.; Chorny, M. Magnetically enhanced cell delivery for accelerating recovery of the endothelium in injured arteries. *Journal of controlled release* 2016, 222, 169-75.

[7]. Vosen, S.; Rieck, S.; Heidsieck, A.; Mykhaylyk, O.; Zimmermann, K.; Bloch, W.; Eberbeck, D.; Plank, C.; Gleich, B.; Pfeifer, A.; Fleischmann, B. K.; Wenzel, D. Vascular Repair by Circumferential Cell Therapy Using Magnetic Nanoparticles and Tailored Magnets. *ACS Nano* 2016, 10 (1), 369-76.

[8]. Riegler, J.; Liew, A.; Hynes, S. O.; Ortega, D.; O'Brien, T.; Day, R. M.; Richards, T.; Sharif, F.; Pankhurst, Q. A.; Lythgoe, M. F. Superparamagnetic iron oxide nanoparticle targeting of MSCs in vascular injury. *Biomaterials* 2013, 34, 1987-94.

[9]. Adams, C. F.; Rai, A.; Sneddon, G.; Yiu, H. H.; Polyak, B.; Chari, D. M. Increasing magnetite contents of polymeric magnetic particles dramatically improves labeling of neural stem cell transplant populations. *Nanomedicine: Nanotechnology, Biology, and Medicine* 2015, 11 (1), 19-29.

[10]. Zohra, F. T.; Medved, M.; Lazareva, N.; Polyak, B. Functional behavior and gene expression of magnetic nanoparticle-loaded primary endothelial cells for targeting vascular stents. *Nanomedicine (Lond)* 2015, 10, 1391-406.

[11]. MacDonald, C.; Friedman, G.; Alamia, J.; Barbee, K.; Polyak, B. Time-varied magnetic field enhances transport of magnetic nanoparticles in viscous gel. *Nanomedicine (Lond)* 2010, 5, 65-76.

[12]. Polyak, B.; Medved, M.; Lazareva, N.; Steele, L.; Patel, T.; Rai, A.; Rotenberg, M. Y.; Wasko, K.; Kohut, A. R.; Sensenig, R.; Friedman, G. Magnetic Nanoparticle-Mediated Targeting of Cell Therapy Reduces In-Stent Stenosis in Injured Arteries. *ACS Nano* 2016, 10 (10), 9559–9569.